Upregulation of EMMPRIN mRNA on sBM substratum

To investigate whether sBM substratum affects the expression of EMMPRIN mRNA in RTE cells, we seeded the 2nd passaged cells on sBM substratum or plastic as the control, and measured the expression of EMMPRIN by quantitative RT-PCR at 24, 36, and 48 h. The RTE cells cultured on sBM substratum demonstrated higher levels of EMMPRIN expression compared to the cells cultured on plastic at 36 h (1.8 ± 0.1SE vs. 0.8 ± 0.1, $p < 0.05$) and 48 h (2.1 ± 0.3 vs. 0.8 ± 0.1, $p < 0.05$) (Fig. 2A).

Diversity in EMMPRIN expression on laminin-111, laminin-332, and type IV collagen

In order to identify what constituent of sBM substratum is responsible for EMMPRIN upregulation, we cultured the 2nd passaged cells on several basement membrane components or plastic as the control. The EMMPRIN expression was significantly upregulated when cultured on laminin-111, compared to that on plastic at 36 h (1.5 ± 0.1 vs. 0.8 ± 0.1, $p < 0.05$) and at 48 h (1.6 ± 0.3 vs. 0.8 ± 0.1, $p < 0.05$) (Fig. 2B). In contrast, the levels of EMMPRIN mRNA expression were not increased on type IV collagen at any time point (Fig. 2C). Furthermore, significant induction of EMMPRIN was not observed on laminin-332, a non-sBM component, at 48 h (0.8 ± 0.04 vs. 1.0 ± 0.02, NS).

Upregulation of TGF-α expression on sBM substratum and laminin-111

Some growth factors are known to increase EMMPRIN expression in corneal epithelial cells [22] and in human breast epithelial cells [23]. Therefore, we wondered whether EGF and/or TGF-α, another ligand of EGF receptor, expression in RTE cells would be affected by sBM substratum or laminin-111, and whether they may indirectly contribute to the upregulation of EMMPRIN. We found that EGF mRNA was undetectable under all conditions tested (data not shown). On the other hand, the expression of TGF-α was significantly upregulated both on sBM substratum (Fig. 3A) and on laminin-111 (Fig. 3B), compared to that on plastic at 36 h (sBM, 1.7 ± 0.3 vs. 1.0 ± 0.1, $p < 0.05$; laminin-111, 2.0 ± 0.1 vs. 1.0 ± 0.1, $p < 0.05$), and at 48 h (sBM, 1.7 ± 0.4 vs. 0.9 ± 0.1, $p < 0.05$; laminin-111, 1.8 ± 0.2 vs. 0.9 ± 0.1, $p < 0.05$), but not on type IV collagen (data not shown). The patterns of induction for TGF-α were similar to those for EMMPRIN.

Difference in morphological phenotypes of RTE cells cultured on sBM substratum, laminin-111, type IV collagen, and plastic

When we seeded the 2nd passaged cells, we found that most of the cells were attached to sBM substratum, whereas only a small portion of the cells were attached to

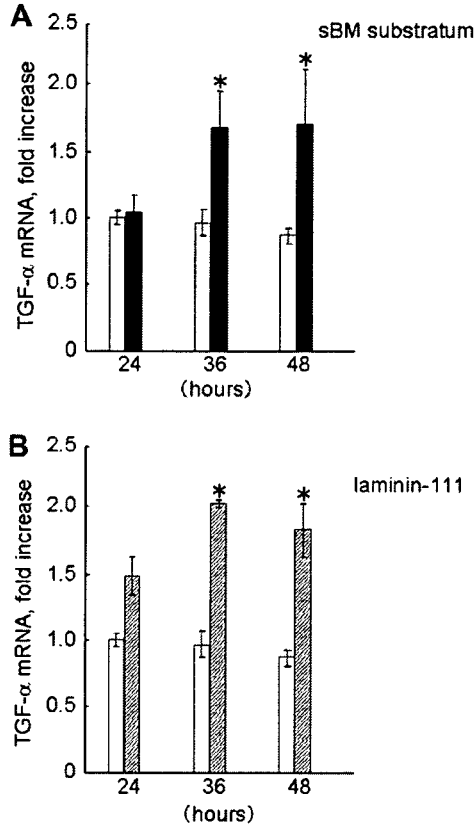

Fig. 3. Expression of TGF- α on sBM substratum and laminin-111. The 2nd passaged cells were cultured on either sBM substratum (black bar) (A), laminin-111 (hatched bars) (B), or plastic (white bars) for 24, 36, or 48 h. "Fold increase" refers to TGF-α mRNA levels detected under each condition at the indicated time points compared to those in culture on plastic for 24 h. $^*p < 0.05$ vs. plastic at each time point.

laminin-111, type IV collagen, or plastic. Consequently, the cells on sBM substratum proliferated more rapidly than those on the other substrata. By phase contrast microscopy, the cells were morphologically flat and sparse on plastic, type IV collagen, and laminin-111 at 48 h (Supplementary Fig. 1A–C). In contrast, the cells were spindle or cuboidal-shaped and were in tightly contact with each other on sBM substratum at 48 h (Supplementary Fig. 1D). These findings suggested that only sBM substratum markedly facilitated cell attachment and consequent cell growth, whereas laminin-111 and the other substrata did not.

Membranous localization of EMMPRIN in RTE cells cultured on laminin-111

The cellular localization of EMMPRIN was examined in the 2nd passaged cells on laminin-111 by immunocytochemistry. EMMPRIN was preferentially observed at cell–cell contact sites in the cells cultured on laminin-111 (Supplementary Fig. 2), indicating that membranous

EMMPRIN is present even in the flat cells cultured on laminin-111.

No increase in MMP-9 in RTE cells cultured on sBM substratum

EMMPRIN is known to induce expression of various MMPs by mesenchymal cells and epithelial cells *in vitro* [8,9], and thus we examined whether MMP-9 expression is also increased on sBM substratum or laminin-111 along with the upregulation of EMMPRIN by the 2nd passaged cells. MMP-9 was not upregulated in either culture on the sBM substratum or laminin-111, compared to that on plastic (Fig. 4A and B). On the other hand, the expression of MMP-9 was significantly upregulated on type IV collagen, compared to that on plastic at 36 h (1.7 ± 0.1 vs. 0.9 ± 0.1, $p < 0.05$), and at 48 h (2.5 ± 0.7 vs. 0.7 ± 0.2, $p < 0.05$) (Fig. 4C). By gelatin zymography, conditioned medium of the 2nd passaged cells demonstrated a band with molecular masses of ~92 kDa, corresponding to pro-MMP-9 [24]. The intensity of the band was higher in the conditioned medium of the cells on type IV collagen, compared to that on plastic, laminin-111 or sBM substratum (Fig. 4D). Taken together, these data indicate that EMMPRIN and MMP-9 are independently regulated by various component of basement membrane.

Discussion

We demonstrated that EMMPRIN is upregulated in RTE cells when cultured on sBM substratum or laminin-111. This implies that the laminin-111 incorporated in the sBM substratum is responsible for stimulating the signals that induce EMMPRIN in those cells. Laminin-111 prefer-

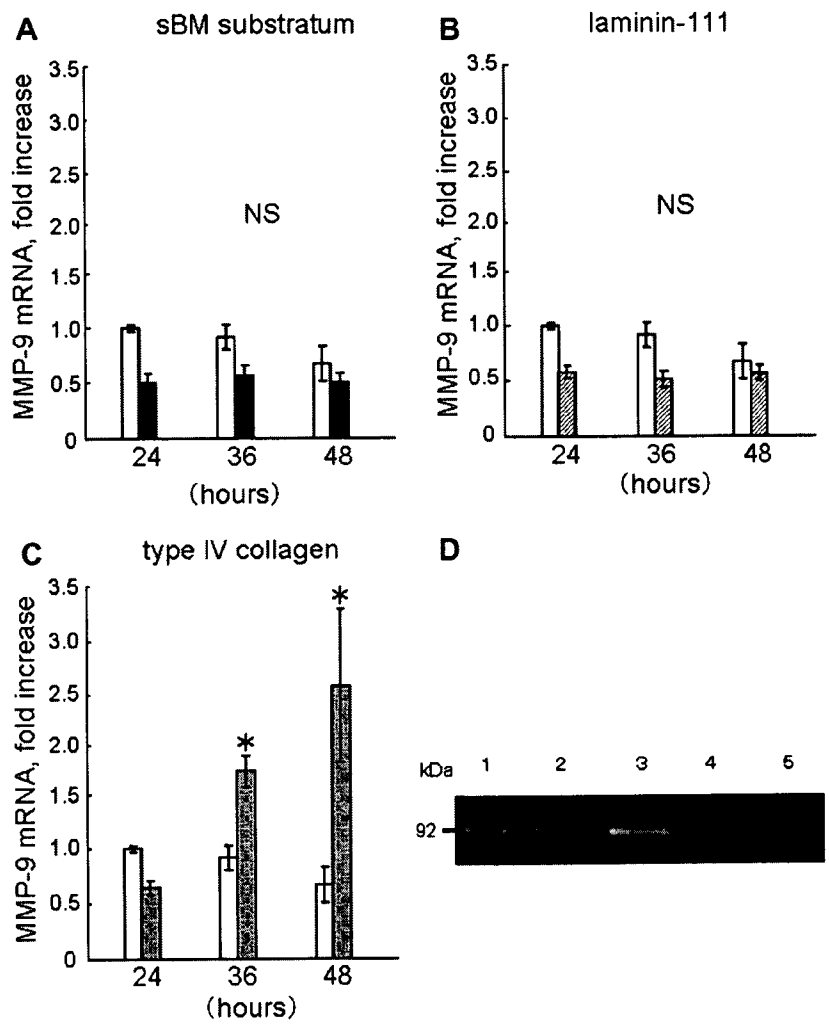

Fig. 4. Expression of MMP-9 on sBM substratum, laminin-111 and type IV collagen. The 2nd passaged cells were cultured on either sBM substratum (black bar) (A), laminin-111 (hatched bars) (B), type IV collagen (shaded bars) (C), or plastic (white bars) for 24, 36, or 48 h. "Fold increase" refers to MMP-9 mRNA levels detected under each condition at the indicated time points compared to those in culture on plastic for 24 h. $^*p < 0.05$ vs. plastic at each time point. Gelatin zymography of the conditioned medium under each culture condition (D). Pro-MMP-9 standard sample (lane 1), conditioned media on plastic (lane 2), type IV collagen (lane 3), laminin-111 (lane 4), and sBM substratum (lane 5) showed gelatinolytic activity at 92 kDa corresponding to pro-MMP-9.

entially induces cell membrane-associated EMMPRIN at cell–cell contact sites, although it does not facilitate rapid cell growth, suggesting that this effect is not through the regulation of cell growth related phenotypes. However, the mechanisms of EMMPRIN upregulation on laminin-111 and on sBM substratum may in fact differ. It is possible that with time in culture on laminin-111 the cells modify the laminin-111 by secreting and depositing other kinds of extracellular matrices and/or growth factors, but not on either laminin-332 or type IV collagen.

Laminins are a major family among basement membrane components: each isoform is composed of α-, β-, and γ-subunits and joined together through a coiled-coil domain [16]. Sixteen laminin isoforms exist, assembled from various combinations of 5α, 3β, and 3γ chains [16]. Temporal expression of specific laminin α chains during lung development is intriguing and not fully understood [15]. According to the coincidental limited expressions of EMMPRIN and laminin-111 (α1β1γ1-subunit composition) at the early stage of lung morphogenesis, laminin-111 may at least partially regulate the induction of EMMPRIN in embryonic lungs. It should also be noted that sBM substratum and laminin-111 are not normally present in adult RTE cells *in vivo*, or even in the setting of injury. On the other hand, EMMPRIN was not induced in the cells cultured on laminin-332 (α3β3γ2-subunit composition), or type IV collagen. These findings are understandable since laminin-332 and type IV collagen are ubiquitously expressed in normal adult lungs [17,25], whereas EMMPRIN is distinctly absent.

Transforming growth factor-β (TGF-β) and EGF have been known to upregulate EMMPRIN expression in corneal epithelial cells [22] and in human breast epithelial cells [23]. Eventually, sBM substratum contains various growth factors [19], and we found that TGF-α, one of the ligands of EGF receptor, was also upregulated by laminin-111 and sBM substratum in the RTE cells accompanied with EMMPRIN upregulation. Taken together, growth factors may directly or indirectly contribute to basement membrane-induced EMMPRIN upregulation in RTE cells.

Unexpectedly, EMMPRIN upregulation was not accompanied by upregulation of MMP-9 when RTE cells were cultured on sBM substratum or laminin-111. One possible explanation is factors which post-transcriptionally suppress the ability of EMMPRIN to induce MMP-9. On the other hand, MMP-9 was upregulated on type IV collagen, which is in line with the previous findings by Yao et al. that human bronchial epithelial cells induce MMP-9 on type IV collagen [26], however, it turned out that this upregulation was clearly independent of EMMPRIN upregulation. EMMPRIN is highly expressed in lung only on embryonic days 13.5 and 15.5 in mice [3], while MMP-9 is absent on those days and upregulated after birth, indicating that the period of EMMPRIN expression does not match that of MMP-9 in murine lung development [4].

In conclusion, we found that sBM substratum and laminin-111 induce EMMPRIN and TGF-α in RTE cells. However, the EMMPRIN upregulation was not accompanied by the induction or release of MMP-9 in those cells. This is the first study to demonstrate the potential roles of basement membrane in transcriptional regulation of EMMPRIN.

Acknowledgments

The authors thank Akiko Furuyama for invaluable advice, Keiko Ohgomori for preparation of sBM substratum, Kazuko Katagiri for gelatin zymography, and Yoko Suzuki for excellent technical assistance with RT-PCR.

Appendix A. Supplementary data

Supplementary data associated with this article can be found, in the online version, at doi:10.1016/j.bbrc.2008.01.105.

References

[1] T. Miyauchi, T. Kanekura, A. Yamaoka, M. Ozawa, S. Miyazawa, T. Muramatsu, Basigin, a new, broadly distributed member of the immunoglobulin superfamily, has strong homology with both the immunoglobulin V domain and the β-chain of major histocompatibility complex class II antigen, J. Biochem. (Tokyo) 107 (1990) 316–323.

[2] C. Biswas, Y. Zhang, R. DeCastro, H. Guo, T. Nakamura, H. Kataoka, K. Nabeshima, The human tumor cell-derived collagenase stimulatory factor (renamed EMMPRIN) is a member of the immunoglobulin superfamily, Cancer Res. 55 (1995) 434–439.

[3] Q.W. Fan, K. Kadomatsu, K. Uchimura, T. Muramatsu, Embigin/basigin subgroup of the immunoglobulin superfamily: different modes of expression during mouse embryogenesis and correlated expression with carbohydrate antigenic markers, Dev. Growth Differ. 40 (1998) 277–286.

[4] K.J. Greenlee, Z. Werb, F. Kheradmand, Matrix metalloproteinases in lung: multiple, multifarious, and multifaceted, Physiol. Rev. 87 (2007) 69–98.

[5] S. Caudroy, M. Polette, J.M. Tournier, H. Burlet, B. Toole, S. Zucker, P. Birembaut, Expression of the extracellular matrix metalloproteinase inducer (EMMPRIN) and the matrix metalloproteinase-2 in bronchopulmonary and breast lesions, J. Histochem. Cytochem. 47 (1999) 1575–1580.

[6] N. Hakuma, T. Betsuyaku, I. Kinoshita, T. Itoh, K. Kaga, S. Kondo, M. Nishimura, H. Dosaka-Akita, High incidence of extracellular matrix metalloproteinase inducer (EMMPRIN) expression in non-small cell lung cancers: association with clinicopathological parameters, Oncology 72 (2007) 197–204.

[7] K. Nabeshima, H. Iwasaki, K. Koga, H. Hojo, J. Suzumiya, M. Kikuchi, EMMPRIN (basigin/CD147): matrix metalloproteinase modulator and multifunctional cell recognition molecule that plays a critical role in cancer progression, Pathol. Int. 56 (2006) 359–367.

[8] S. Zucker, M. Hymowitz, E.E. Rollo, R. Mann, C.E. Conner, J. Cao, H.D. Foda, D.C. Tompkins, B.P. Toole, Tumorigenic potential of extracellular matrix metalloproteinase inducer, Am. J. Pathol. 158 (2001) 1921–1928.

[9] T. Sameshima, K. Nabeshima, B.P. Toole, K. Yokogami, Y. Okada, T. Goya, M. Koono, S. Wakisaka, Glioma cell extracellular matrix metalloproteinase inducer (EMMPRIN) (CD147) stimulates production of membrane-type matrix metalloproteinases and activated gelatinase A in co-cultures with brain-derived fibroblasts, Cancer Lett. 157 (2000) 177–184.

[10] T. Betsuyaku, M. Tanino, K. Nagai, Y. Nasuhara, M. Nishimura, R.M. Senior, Extracellular matrix metalloproteinase inducer is increased in smokers' bronchoalveolar lavage fluid, Am. J. Respir. Crit. Care Med. 168 (2003) 222–227.
[11] T. Betsuyaku, K. Kadomatsu, G.L. Griffin, T. Muramatsu, R.M. Senior, Increased basigin in bleomycin-induced lung injury, Am. J. Respir. Cell Mol. Biol. 28 (2003) 600–606.
[12] N. Odajima, T. Betsuyaku, Y. Nasuhara, T. Itoh, Y. Fukuda, R.M. Senior, M. Nishimura, Extracellular matrix metalloproteinase inducer in interstitial pneumonias, Hum. Pathol. 37 (2006) 1058–1065.
[13] P.D. Yurchenco, J.C. Schittny, Molecular architecture of basement membranes, FASEB J. 4 (1990) 1577–1590.
[14] J.H. Miner, P.D. Yurchenco, Laminin functions in tissue morphogenesis, Annu. Rev. Cell Dev. Biol. 20 (2004) 255–284.
[15] N.M. Nguyen, R.M. Senior, Laminin isoforms and lung development: all isoforms are not equal, Dev. Biol. 294 (2006) 271–279.
[16] M. Aumailley, L. Bruckner-Tuderman, W.G. Carter, R. Deutzmann, D. Edgar, P. Ekblom, J. Engel, E. Engvall, E. Hohenester, J.C.R. Jones, H.K. Kleinman, M.P. Marinkovich, G.R. Martin, U. Mayer, G. Meneguzzi, J.H. Miner, K. Miyazaki, M. Patarroyo, M. Paulsson, V. Quaranta, J.R. Sanes, T. Sasaki, K. Sekiguchi, L.M. Sorokin, J.F. Talts, K. Tryggvason, J. Uitto, I. Virtanen, K. von der Mark, U.M. Wewer, Y. Yamada, P.D. Yurchenco, A simplified laminin nomenclature, Matrix Biol. 24 (2005) 326–332.
[17] C. Coraux, G. Meneguzzi, P. Rousselle, E. Puchelle, D. Gaillard, Distribution of laminin 5, integrin receptors, and branching morphogenesis during human fetal lung development, Dev. Dyn. 225 (2002) 176–185.
[18] A. Furuyama, K. Mochitate, Assembly of the exogenous extracellular matrix during basement membrane formation by alveolar epithelial cells in vitro, J. Cell Sci. 113 (2000) 859–868.
[19] T. Hosokawa, A. Furuyama, K. Katagiri, T. Betsuyaku, M. Nishimura, K. Mochitate, Differentiation of tracheal basal cells to ciliated cells and tissue reconstruction on the synthesized basement membrane substratum *in vitro*, Connect. Tissue Res. 48 (2007) 9–18.
[20] T. Hoshiba, K. Mochitate, T. Akaike, Hepatocytes maintain their function on basement membrane formed by epithelial cells, Biochem. Biophys. Res. Commun. 359 (2007) 151–156.
[21] T. Betsuyaku, M. Nishimura, K. Takeyabu, M. Tanino, P. Venge, S. Xu, Y. Kawakami, Neutrophil granule proteins in bronchoalveolar lavage fluid from subjects with subclinical emphysema, Am. J. Respir. Crit. Care Med. 159 (1999) 1985–1991.
[22] E.E. Gabison, S. Mourah, E. Steinfels, L. Yan, T. Hoang-Xuan, M.A. Watsky, B. De Wever, F. Calvo, A. Mauviel, S. Manashi, Defferential expression of extracellular matrix metalloproteinase inducer (CD147) in normal and ulcerated corneas: role in epitheliostromal interactions and matrix metalloproteinase induction, Am. J. Pathol. 166 (2005) 209–219.
[23] S. Menashi, M. Serova, L. Ma, S. Vignot, S. Mourah, F. Calvo, Regulation of extracellular matrix metalloproteinase inducer and matrix metalloproteinase expression by amphiregulin in transformed human breast epithelial cells, Cancer Res. 63 (2003) 7575–7580.
[24] A. Pardo, R. Barrios, V. Maldonado, J. Melendez, J. Perez, V. Ruiz, L. Segura-Valdez, J.I. Sznajder, M. Selman, Gelatinases A and B are up-regulated in rat lungs by subacute hyperoxia, Am. J. Pathol. 153 (1998) 833–844.
[25] T.J. Mariani, J.J. Reed, S.D. Shapiro, Expression profiling of the developing mouse lung insights into the establishment of the extracellular matrix, Am. J. Respir. Cell Mol. Biol. 26 (2002) 541–548.
[26] P.M. Yao, C. Delclaux, M.P. d'Ortho, B. Maitre, A. Harf, C. Lafuma, Cell–matrix interactions modulate 92-kDa gelatinase expression by human bronchial epithelial cells, Am. J. Respr. Cell Mol. Biol. 18 (1998) 813–822.

Respiratory Research

BioMed Central

Research

Open Access

Bronchiolar chemokine expression is different after single versus repeated cigarette smoke exposure

Tomoko Betsuyaku*[1], Ichiro Hamamura[2], Junko Hata[2], Hiroshi Takahashi[2], Hiroaki Mitsuhashi[2], Tracy L Adair-Kirk[3], Robert M Senior[3] and Masaharu Nishimura[1]

Address: [1]First Department of Medicine, Hokkaido University School of Medicine, Kita-15, Nishi-7, Kita-ku, Sapporo, 060-8683, Japan, [2]Teijin Institute for Bio-medical Research, Teijin Pharma Ltd., 4-3-2 Asahigaoka, Hino, Tokyo 191-8512, Japan and [3]Division of Pulmonary and Critical Care Medicine, Department of Medicine, Washington University School of Medicine and Barnes-Jewish Hospital, 660 So. Euclid Avenue St. Louis, MO 63110, USA

Email: Tomoko Betsuyaku* - bytomoko@med.hokudai.ac.jp; Ichiro Hamamura - ichiro.hamamura@tech.mrc.ac.uk; Junko Hata - j.hata@teijin.co.jp; Hiroshi Takahashi - hiros.takahashi@teijin.co.jp; Hiroaki Mitsuhashi - h.mitsuhashi@teijin.co.jp; Tracy L Adair-Kirk - tkirk@im.wustl.edu; Robert M Senior - seniorr@msnotes.wustl.edu; Masaharu Nishimura - ma-nishi@med.hokudai.ac.jp

* Corresponding author

Published: 21 January 2008

Respiratory Research 2008, 9:7 doi:10.1186/1465-9921-9-7

Received: 3 September 2007

Accepted: 21 January 2008

This article is available from: http://respiratory-research.com/content/9/1/7

Abstract

Background: Bronchioles are critical zones in cigarette smoke (CS)-induced lung inflammation. However, there have been few studies on the *in vivo* dynamics of cytokine gene expression in bronchiolar epithelial cells in response to CS.

Methods: We subjected C57BL/6J mice to CS (whole body exposure, 90 min/day) for various periods, and used laser capture microdissection to isolate bronchiolar epithelial cells for analysis of mRNA by quantitative reverse transcription-polymerase chain reaction.

Results: We detected enhanced expression of keratinocyte-derived chemokine (KC), macrophage inflammatory protein-2 (MIP-2), tumor necrosis factor-α (TNF-α), and interleukin-1β (IL-1β) by bronchial epithelial cells after 10 consecutive days of CS exposure. This was mirrored by increases in neutrophils and KC, MIP-2, TNF-α, and IL-1β proteins in the bronchoalveolar lavage (BAL) fluid. The initial inhalation of CS resulted in rapid and robust upregulation of KC and MIP-2 with concomitant DNA oxidation within 1 hr, followed by a return to control values within 3 hrs. In contrast, after CS exposure for 10 days, this initial surge was not observed. As the CS exposure was extended to 4, 12, 18 and 24 weeks, the bronchiolar KC and MIP-2 expression and their levels in BAL fluid were relatively dampened compared to those at 10 days. However, neutrophils in BAL fluid continuously increased up to 24 weeks, suggesting that neutrophil accumulation as a result of long-term CS exposure became independent of KC and MIP-2.

Conclusion: These findings indicate variable patterns of bronchiolar epithelial cytokine expression depending on the duration of CS exposure, and that complex mechanisms govern bronchiolar molecular dynamics *in vivo*.

Background

Chronic obstructive pulmonary disease (COPD) is characterized by irreversible airflow limitation due to structural alterations of the small airways, chronic inflammation in the airways and alveolar spaces, and loss of elastic recoil caused by destruction of lung parenchyma. Since the pathology of COPD is that of a chronic inflammatory process, many studies have focused on identifying the inflammatory cell types and/or cytokines that play a role in this condition. Increased numbers of neutrophils, macrophages, and lymphocytes in the airways are found associated with COPD [1-3], and various mediators derived from these cells, such as interleukin (IL)-1β, IL-6, IL-8, tumor necrosis factor (TNF)-α, monocyte chemoattractant protein (MCP-1), and matrix metalloproteinase (MMP)-2, MMP-8, and MMP-9, are suggested to contribute to the development of COPD [4,5].

Cigarette smoke (CS) is the main risk factor for the development of COPD. Oxidative stress caused by CS can injure lung cells directly and can trigger cytokine production, leading to the recruitment of inflammatory cells into the lungs [6-8]. The induction of these cytokines is regulated by the activation of redox-sensitive transcription factors, such as nuclear factor-kappa B (NF-κB) [9,10]. Increased expression of NF-κB has been detected in the airway epithelium of smokers compared to non-smokers [11].

Airway epithelium is an important site of cytokine expression in COPD and in response to CS [12,13]. For example, cultured airway epithelial cells produce IL-6 and IL-8 in response to CS exposure [14-16], and TNF-α, IL-8, MCP-1, and macrophage inflammatory protein (MIP)-1α are upregulated in the bronchiolar epithelium of subjects with COPD [17-19]. However, there is scant data on the time course of cytokine responses to CS by airway epithelium. Therefore, we decided to examine the temporal relationship of airway epithelial cytokine production after CS exposure *in vivo* utilizing a mouse model of mainstream CS exposure.

We hypothesized that CS would induce changes in gene expression of pro-inflammatory cytokines, and that the kinetics of the response would differ depending on duration of exposure and the cytokine. Accordingly, we examined the expression of keratinocyte-derived chemokine (KC)/CXCL1 and MIP-2/CXCL2, the combined functional homologues to human IL-8, as well as TNF-α and IL-1β by bronchiolar epithelial cells following either a single CS exposure, repeated exposures for 10 days, or repeated exposure for 24 weeks. We have identified previously unrecognized dynamics in gene expression in bronchiolar epithelium *in vivo* following CS exposure.

Methods

CS Exposure

Male C57BL/6J mice, 9–10 weeks of age (Charles River, Atsugi, Japan), were exposed to whole body mainstream CS generated from commercially available filtered cigarettes (12 mg tar/1.0 mg nicotine, Philip Morris, Richmond, VA) by the INH06-CIGR0A smoking system (MIPS Co., Osaka, Japan) using the following parameters: 15.5 puff/min/cigarette; air flow, 0.07 L/min; and volume, 280 mL/second, as described elsewhere [20]. The CS was diluted with filtered air at 1:7 ratio and directed into the exposure chamber (50(L) × 50(W) × 25(H) cm) at a smoke to air ratio of 1:2. The box was fitted with an exhaust vent of the same size as a blower vent in order to avoid the accumulation of mainstream smoke. In initial experiments, mice were exposed to CS for 90 min per day for 1, 3, 7 or 10 days, and were sacrificed 24 hrs after the last CS exposure. For assessment of kinetic patterns in gene expression following CS exposure, mice received either a single 90-min CS exposure or daily exposure for 10 days, and then were sacrificed at 1, 3, 6 or 24 hrs after the last CS exposure. In long-tem CS exposure experiments, mice were exposed to CS for 90 min per day, 6 days per week, for 4, 12, 18 or 24 weeks, and were sacrificed 24 hrs after the last CS exposure. Age-matched, air-exposed mice served as controls. All animal procedures were performed in accordance with the regulations of the Animal Care and Use Committee of Teijin Institute for Bio-medical Research.

Analysis of plasma cotinine levels

Blood samples were collected at 1 and 3 hrs after the last CS exposure and the levels of cotinine in the plasma were measured using a quantitative enzyme immunoassay kit (Salimetrics, State College, PA), as described previously [21]. Data represent average concentration from 3 mice per condition performed in duplicate.

Collection of Broncholalveolar Lavage (BAL) fluid

At various times after CS exposure, mice were anesthetized with urethane and α-chloralose and then exsanguinated by severing the abdominal aorta, and BAL fluid was retrieved by injecting 1.0 ml saline through the trachea as described previously [22]. An aliquot of each BAL fluid was mixed with an equal volume of Turk's solution (Wako, Osaka, Japan) and the total cell number was determined using a hemocytometer. Differential cell counts were performed on Diff-Quik™ (International Reagents, Kobe, Japan)-stained cytospin preparations. Data represent the average numbers of cells per ml of BAL fluid from 8 mice per condition. The BAL fluid was centrifuged, and the cell-free supernatants were stored at -80°C until use.

Detection of albumin, MIP-2, KC, TNF-α, and IL-1β in BAL fluid

The concentration of albumin in BAL fluid was determined using an albumin B test-Wako kit (Wako) according to manufacturer's protocol. The quantity of KC, MIP-2, TNF-α, and IL-1β in the BAL fluid was determined by ELISA kits (R&D Systems, Minneapolis, MN) according to manufacturer's protocols. The detection limit was 7 pg/mL for KC, MIP-2 and IL-1β, and 15 pg/mL for TNF-α. Data represent the average concentration of 8 mice per condition performed in duplicate.

Immunohistochemical evaluation of DNA oxidation in the lung

Lungs were inflated with diluted Tissue-Tek OCT (Sakura Finetek U.S.A., Torrance, CA) (50% vol/vol in ribonuclease (RNase)-free PBS containing 10% sucrose) and immediately frozen on dry ice as previously described [23]. Antigen retrieval was done on 5 μm sections by incubating in L.A.B. solution (Polysciences, Warrington, PA) at room temperature for 10 min. Sections were incubated with 3% bovine serum albumin (Sigma, St. Louis, MO) and the mouse immunoglobulin blocking reagent from the M.O.M. immunodetection kit (Vector Laboratories, Burlingame, CA) in the TNB solution included in the TSA Biotin System Immunohistochemistry kit (PerkinElmer Life and Analytical Sciences, Wellesley, MA) for 30 min in order to block non-specific binding. Sections were then incubated with the mouse monoclonal anti-8-hydroxy-2'-deoxyguanosine (8-OHdG) antibody (10 μg/mL) (Japan Institute for the Control of Aging, Shizuoka, Japan) for 1 hr at room temperature, followed by 3% hydrogen peroxide for 10 min at room temperature [24]. Immunostaining was developed using the M.O.M. detection kit (Vector Laboratories) with DAB substrate and counterstained with Mayer's hematoxylin.

Collection of bronchiolar epithelial cells by Laser Capture Microdissection (LCM)

LCM was performed on 7 μm frozen sections to retrieve cells within 100 μm of the bronchoalveolar junction using the PixCell II System (Arcturus Engineering, Mountain View, CA) with the following parameters: laser diameter, 30 μm; pulse duration, 5 ms; and amplitude, 50 mW, as described previously [23]. Approximately 10,000 laser bursts were used to collect cells for RNA isolation from each mouse.

RNA isolation and real-time RT-PCR

Total RNA was extracted from LCM-retrieved bronchiolar epithelial cells using an RNeasy Mini kit (Qiagen, Hilden, Germany), or from whole lung homogenates using the ISOGEN RNA isolation kit (Nippon Gene Co. Ltd. Toyama, Japan). The quantity and quality of RNA were determined using an RNA LabChip kit (Agilent Technologies, Palo Alto, CA) or a NanoDrop spectrophotometer (NanoDrop Inc., Wilmington, DE). RNA was reverse transcribed using TaqMan Reverse Transcription Reagents kit (Applied Biosystems, Foster City, CA) as described previously [25]. The resulting first-strand cDNAs were used as templates for quantitative real-time RT-PCR using the ABI Prism 7700 Sequence Detector (Applied Biosystems) and gene-specific TaqMan Gene Expression Assays probes (Applied Biosystems) as described previously [18]. Probes for mouse KC (Assay ID: Mm00433859_m1) were derived from the boundary of exons 3 and 4 of the murine KC gene [26]. Probes for mouse MIP-2 (Mm00436450_m1) were derived from the boundary of exons 3 and 4 of the murine MIP-2 gene [27]. Probes for mouse TNF-α (Mm00443258_m1) were derived from the boundary of exons 1 and 2 of the murine TNF-α gene [28]. Probes for mouse IL-1β (Mm00434228_m1) were derived from the boundary of exons 3 and 4 of the murine IL-1β gene [29]. Probes for mouse β2-macroglobulin (β2-MG; Mm00437764_m1) were used as an endogenous control as described previously [25]. The relative amounts of each mRNA in the samples were assessed by interpolation of their cycle thresholds from a standard curve, and were then normalized against β2-MG mRNA. RT-PCR data represent 6–12 mice per condition performed in triplicate.

Statistical analysis

All results are reported as means ± standard error of the mean (SEM). Statistical significance of the values at each time point after CS exposure was evaluated by Dunnett's type multiple comparative analyses against the values in pretreatment groups. Differences were considered significant at $p < 0.05$. Statistical analyses were performed using SAS version 8.2 for Windows XP (SAS Institute, Tokyo, Japan).

Results

CS Exposure

To confirm adequate CS exposure, the levels of plasma cotinine were measured. Cotinine was essentially undetectable in mice unexposed to CS (<5 ng/mL) (Figure 1A). However, following a single 90-min CS exposure, a dramatic increase in plasma cotinine levels was detected within 1 hr of CS exposure, which was reduced but still elevated 3 hr after CS exposure. Exposure of mice to CS for 10 consecutive days did induce a slight progressive increase of cotinine in the plasma. The levels of plasma cotinine in our studies are similar to that detected in blood samples of ICR mice following CS exposure [30] and in blood samples of humans who smoke >5 cigarettes a day [31].

BAL fluid albumin, a biomarker of tissue injury, was also measured. A significant increase in albumin in the BAL fluid was detected after 3 days of CS exposure, compared

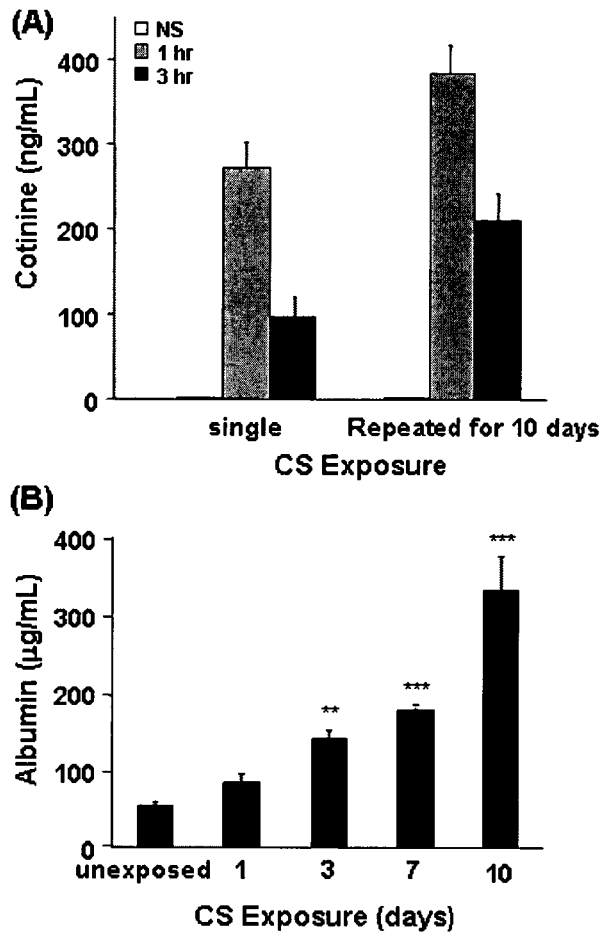

Figure 1

Plasma cotinine and BAL albumin levels are elevated following CS exposure. *(A)* Blood samples were collected at 1 and 3 hrs after the last CS exposure and the levels of cotinine in the plasma was measured using a quantitative enzyme immunoassay kit. Data represent average concentration of three mice per condition ± SEM. *(B)* BAL fluids were collected at 24 hr after the last CS exposure and assayed for the presence of albumin using the albumin B test-Wako kit. Data represent the average concentration of eight mice per condition ± SEM. Statistical significance: ** = $p < 0.01$; *** = $p < 0.001$.

to levels in unexposed controls (Figure 1B). The levels of albumin in the BAL fluid continued to increase following 10 consecutive days of CS exposures. These data indicate that the conditions for CS exposure utilized for these studies were sufficient to induce known effects caused by mainstream CS exposure [30,32,33].

CS-induced DNA oxidative stress in bronchiolar and alveolar epithelium

To determine whether CS exposure induces oxidative stress in lung cells, sections were immunostained for 8-OHdG, a marker of oxidative DNA stress. Oxidative stress was not detected in the lungs of mice unexposed to CS (Figure 2A). Within 1 hr after a single 90-min CS exposure, nuclear staining of 8-OHdG was markedly increased in the bronchiolar and alveolar type II epithelial cells (Figure 2B), confirming that both cell types are major targets of CS oxidants. However, 24 hr after a single CS exposure, the staining was back almost to baseline (Figure 2C). These data are consistent with the findings of Aoshiba *et al.* [34] who examined the kinetics of oxidative stress in mice following a single CS exposure.

Surprisingly, after repeated CS exposure for 10 days, nuclear staining of 8-OHdG was not detected in the bronchiolar or alveolar epithelium either before (Figure 2D) or at 1 hr (Figure 2E) following the final CS exposure. In long-tem CS exposure experiments (4 or 24 weeks), 8-OHdG staining was not observed at 4 or 24 weeks, either (data not shown). Normal mouse IgG1 negative control (DakoCytomation, Glostrup, Denmark) in place of the 8-OHdG antibody resulted in no tissue staining (Figure 2F). These data suggest that repeated CS exposure elicits a mechanism in airway and alveolar epithelial cells to protect against DNA oxidative stress.

Inflammatory cells in BAL fluid during 10 days of CS exposure

To determine whether short-term CS exposure elicits an inflammatory response, mice were exposed to CS for up to 10 days and the BAL fluids collected 24 hr after the last CS exposure were examined for the presence of inflammatory cells. After 10 days of CS exposure, the total number of cells in the BAL fluid was significantly increased compared to the BAL fluid of unexposed mice (Figure 3A). Although slightly elevated after 3 days of CS exposure, there was no significant change in the number of macrophages in the BAL fluid irrespective of duration of CS exposure (Figure 3B). In contrast, a significant increase in the number of neutrophils in the BAL fluid was observed after 3 days of CS exposure, which continued to increase following consecutive CS exposures (Figure 3C). A significant increase in the number of lymphocytes was also detected after 10 days of CS exposure (Figure 3D). However, based on the total number of cells relative to the number of each cell type in the BAL fluid, the predominant infiltrating cells in response to CS exposure were neutrophils.

Neutrophilic chemokines in BAL fluid during 10 days of CS exposure

Since the primary infiltrating cells in response to CS exposure were neutrophils, we examined the BAL fluid for

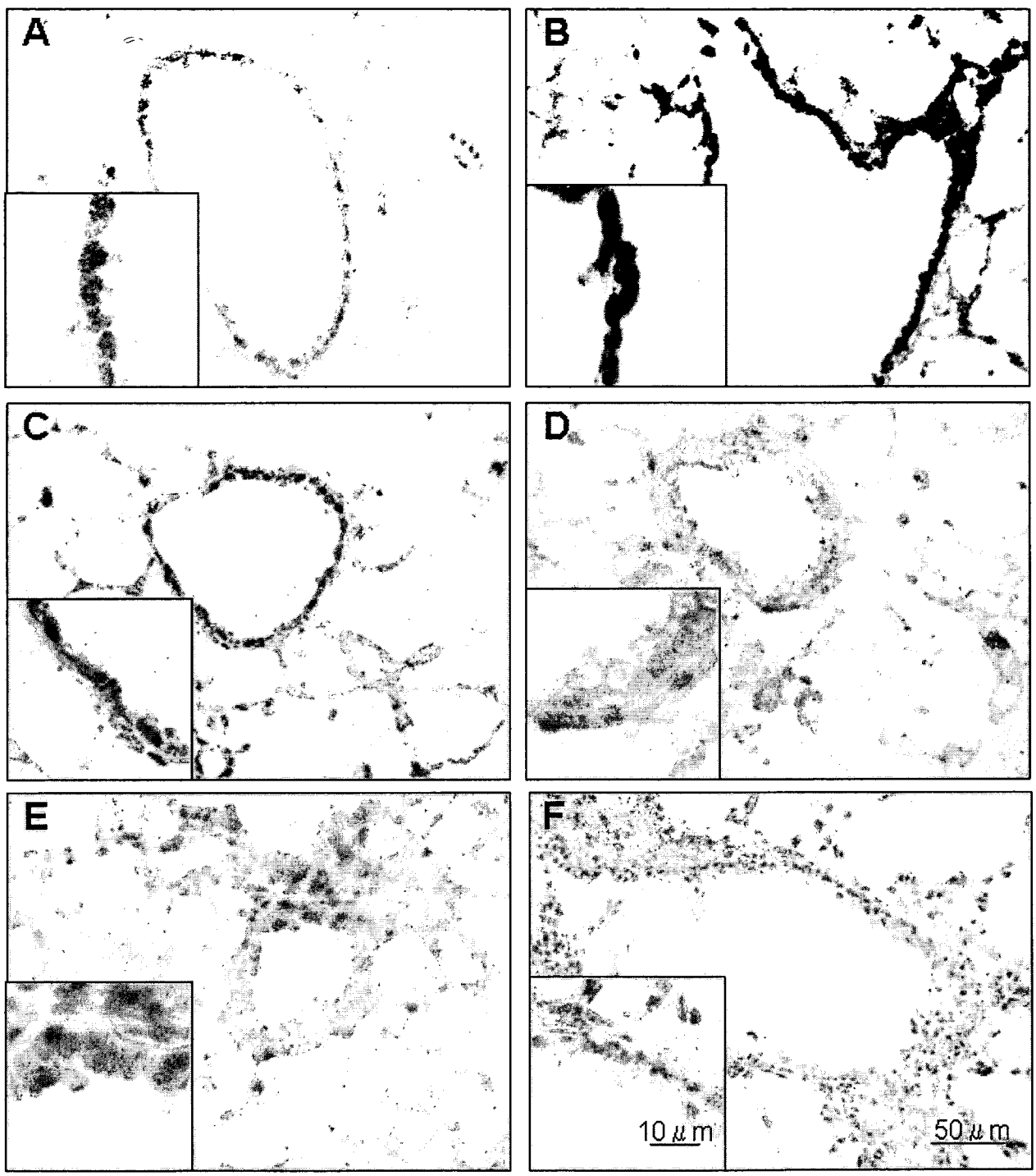

Figure 2
Initial CS exposure induces oxidative stress in airway epithelial cells. Mice were unexposed *(A)*, exposed to a single CS exposure *(B and C)*, or repeatedly exposed to CS for 10 days *(D and E)*. Lung sections were stained for oxidative DNA stress using an anti-8-OHdG antibody at 1 hr *(B and E)* or 24 hrs *(C and D)* following the last CS exposure. Normal mouse IgG1 in place of the 8-OHdG antibody served as a negative control *(F)*. Images are representative of five mice per condition.

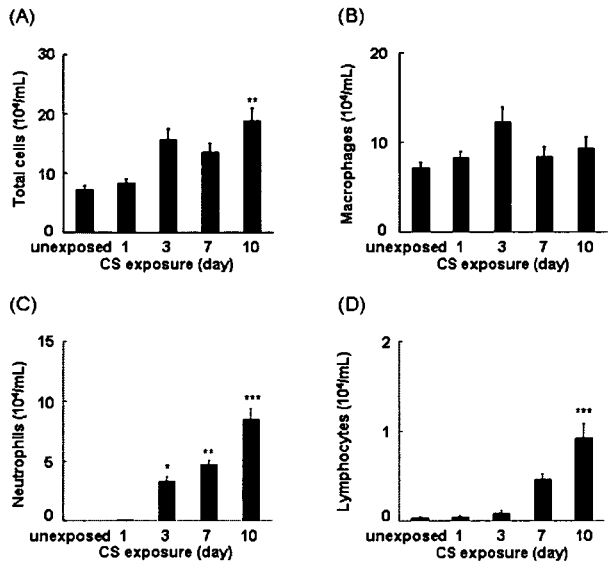

Figure 3
Repeated CS exposure induces inflammatory cell recruitment. Mice were repeatedly exposed to CS for up to 10 days and the cell content in the BAL fluid was identified as described in Materials and Methods. Data represent the average number of total cells *(A)*, macrophages *(B)*, neutrophils *(C)*, and lymphocytes *(D)* per ml BAL fluid ± SEM from eight mice. Statistical significance: * = $p < 0.05$; ** = $p < 0.01$; *** = $p < 0.001$.

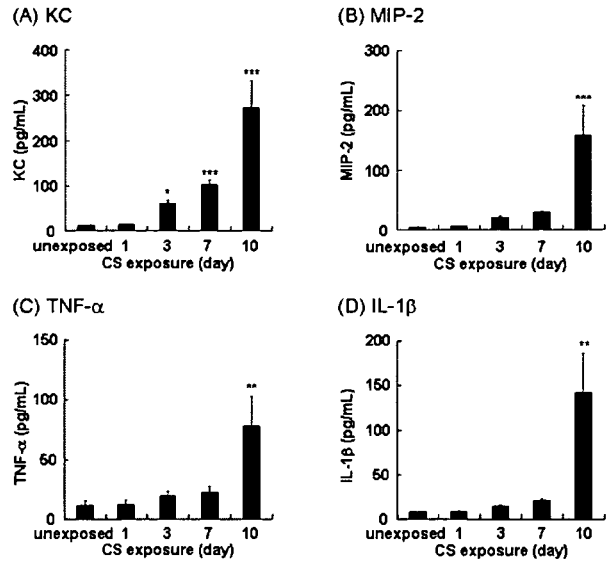

Figure 4
Repeated CS exposure increases KC, MIP-2, TNF-α and IL-1β in BAL fluid. Mice were repeatedly exposed to CS for up to 10 days and the levels of KC *(A)*, MIP-2 *(B)*, TNF-α *(C)* and IL-1β *(D)* in the BAL fluid were determined by ELISA. Data represent the average concentration per ml BAL fluid ± SEM from eight mice. Statistical significance: * = $p < 0.05$; ** = $p < 0.01$; *** = $p < 0.001$.

cytokines that attract neutrophils. After 3 days of CS exposure, a significant increase in the level of KC in the BAL fluid was observed compared to the BAL fluid from unexposed mice (Figure 4A). The levels of KC in the BAL fluid continued to increase following consecutive CS exposures, paralleling the accumulation of neutrophils in the BAL fluid. A significant increase in the levels of MIP-2 (Figure 4B), TNF-α (Figure 4C) and IL-1β (Figure 4D) was also detected after 10 days of CS exposure.

Whole lung and bronchiolar cytokine expression during 10 days of CS exposure

Since CS produced oxidative stress in the airways (Figure 2), we examined whether bronchiolar epithelial cells express cytokines in response to CS by real-time RT-PCR analyses of RNA isolated from LCM-retrieved terminal bronchiolar epithelial cells. Furthermore, we compared the expression levels of KC, MIP-2, TNF-α, and IL-β in LCM-retrieved bronchiolar epithelial cells to the levels in whole lung homogenates. We found that KC was significantly upregulated after a single CS exposure in whole lung homogenates, whereas a significant upregulation in the bronchiolar epithelium was not detected until following 3 days of CS exposure (Figure 5A). The expression of MIP-2 was increased in bronchiolar epithelial cells after 3 and 10 days of CS exposure (Figure 5B). The expression of TNF-α was increased in bronchiolar epithelial cells after 7 and 10 days of CS exposure (Figure 5C). However, the expression of MIP-2 and TNF-α in whole lung homogenates was not significantly increased until after 10 days of CS exposure. Significant upregulation of IL-1β was observed at 10 days in both whole lung homogenates and in bronchiolar epithelium (Figure 5D). Although there are temporal differences in the expression of these cytokines between whole lung homogenates and bronchiolar epithelium, the expression of these genes was notably higher in bronchiolar epithelial cells when compared with whole lung homogenate at all time points.

Patterns of bronchiolar cytokine expression after CS exposure

To determine the dynamics of the bronchiolar epithelial cell cytokine expression, we examined the expression of KC, MIP-2, TNF-α, and IL-1β by the bronchiolar epithelium over a 24-hr period following either a single CS exposure or repeated exposures for 10 days. In bronchiolar epithelial cells of CS-naïve mice, rapid and robust increases in the expression of KC (70-fold) and MIP-2 (20-fold) were observed within 1 hr of a single CS exposure, compared to unexposed mice (Figure 6A and 6B). These values returned close to baseline values within 3

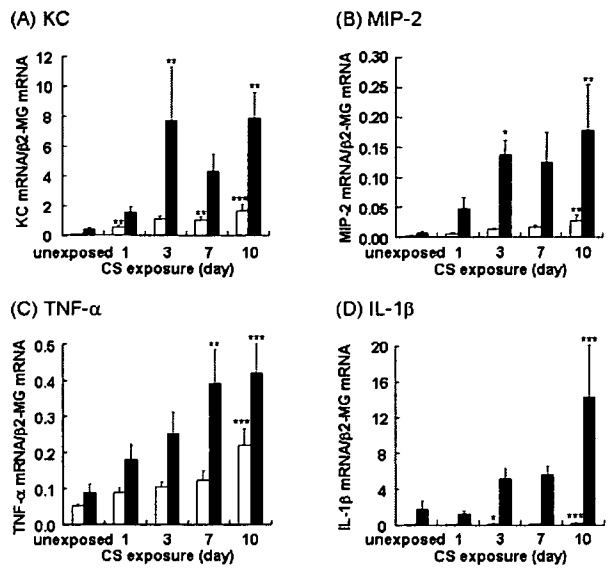

Figure 5

Repeated CS exposure upregulates KC, MIP-2, TNF-α, and IL-1β expression in whole lung homogenate and in LCM-retrieved bronchiolar epithelium. Mice were repeatedly exposed to CS for up to 10 days, and the expression of KC *(A)*, MIP-2 *(B)*, TNF-α *(C)*, and IL-1β *(D)* in whole lung homogenates *(white bars)* and LCM-retrieved bronchiolar epithelium *(black bars)* were determined by real-time RT-PCR. Data represent the average expression relative to β2-MG ± SEM from at least six mice. Statistical significance: * = $p < 0.05$; ** = $p < 0.01$; *** = $p < 0.001$.

hrs. Although the expression of KC and MIP-2 in bronchiolar epithelial cells of mice after 10 days of repeated exposure was elevated before the final CS exposure, a transient increase was not observed after CS exposure.

Similar to KC and MIP-2, but to a much lesser extent (2-fold), an increase in IL-1β expression was detected in the bronchiolar epithelium within 1 hr following a single CS exposure which returned close to baseline levels within 3 hrs (Figure 6D). Also similar to KC and MIP-2, the level of IL-1β expression following repeated CS exposure was elevated before the final CS exposure as compared to baseline levels of CS-naïve mice. However, unlike KC and MIP-2, which were not upregulated in response to the final CS exposure, IL-1β expression slowly rose over the 24 hr period following the final CS exposure.

In contrast to KC, MIP-2, and IL-1β, bronchiolar expression of TNF-α failed to return to baseline by 3 hr after the initial CS exposure (Figure 6C) and after 10 days of repeated exposure, there was a slight, slow increase in TNF-α expression by the bronchiolar epithelium following the final CS exposure. These data indicate that the kinetic patterns of expression of different cytokines by the bronchiolar epithelium following CS exposure vary.

Inflammatory cells in BAL fluid during long-term CS exposure

Thereafter, we addressed whether the pattern of inflammatory response of the lung to CS exposure observed after 10 days persists following long-term CS exposure. We found that as the exposure of CS to the mice was extended to 4, 12, 18 and 24 weeks, a further increase in the total cell number in BAL fluid was observed (Figure 7A). Similarly, the elevated number of neutrophils in BAL fluid that developed during the short-term CS exposure persisted in the long-term CS exposure, showing over 50% neutrophils out of the total BAL cells at 24 weeks (Figure 7B).

KC and MIP-2 in BAL fluid during long-term CS exposure

In contrast to the parallel increase in the number of neutrophils and the levels of KC and MIP-2 in BAL fluid in the short-term CS exposure experiment, KC and MIP-2 levels in BAL fluid declined by 4 weeks of CS exposure compared to the levels at 10 days despite the persistent increase of neutrophils (Figure 8A and 8B).

Bronchiolar KC and MIP-2 expression during long-term CS exposure

As described above, we detected enhanced bronchiolar expression of KC and MIP-2 after 10 consecutive days of CS exposure (Figure 5A and 5B). However, as the exposure of CS to the mice was extended to 4, 12, 18 and 24 weeks, bronchiolar KC and MIP-2 mRNA were nearly back to baseline after 4 weeks of CS exposure and did not change with continued CS exposure up to 24 weeks (Figure 9A and 9B). Bronchiolar KC and MIP-2 expressions exhibited a similar pattern to those levels in BAL fluid (Figure 8A and 8B).

Discussion

Prior animal studies have established the expression of pro-inflammatory cytokines in various types of experimental lung injury including CS-induced models [30,35-39]. However, the role of bronchiolar epithelial cells, specifically, in producing pro-inflammatory cytokines and their inflammatory sequela *in vivo* remains to be elucidated. Several approaches might be used to detect cytokine expression. *In situ* hybridization can provide cell-specific information regarding gene expression, but it is not quantitative. Real-time RT-PCR provides quantitative measure of gene expression, but using RNA from homogenized tissue has the disadvantage of averaging-out signals, in that signals from small, but potentially critical, cell populations could go undetected. The use of LCM to selectively isolate a defined cell population improves the sample preparation for gene expression analysis. Furthermore, the predominance of Clara cells in the distal air-

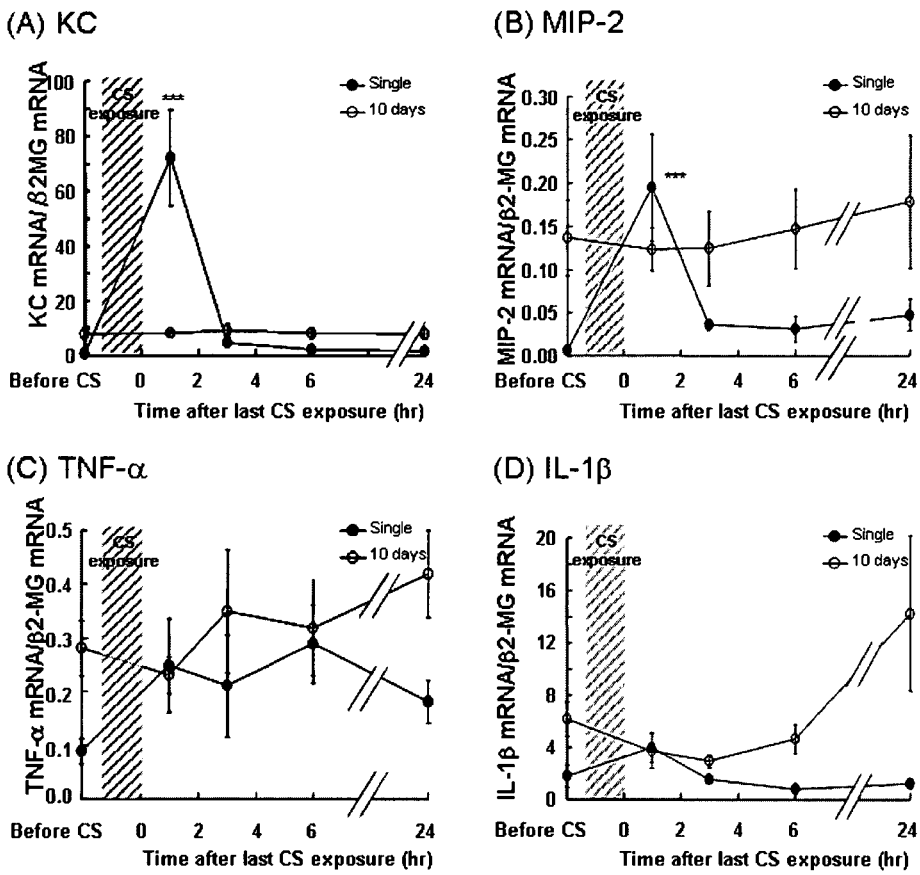

Figure 6

Kinetics in bronchiolar expression of KC and MIP-2 over 24 hrs is different after single vs. repeated CS exposure. Mice were exposed to a single CS exposure *(closed circles)* or repeatedly exposed to CS for 10 days *(open circles)*. For the 10 day exposure the time point before CS represents 24 hrs after 9 days exposure. At various times up to 24 hrs following last CS exposure, the bronchiolar epithelial cells were harvested by LCM and the expression of KC *(A)*, MIP-2 *(B)*, IL-1β *(C)*, and TNF-α *(D)* were determined by real-time RT-PCR. Data represent the average expression relative to β2-MG ± SEM from at least six mice. Statistical significance: *** = $p < 0.001$ vs. before CS exposure at each time point.

ways of mice [40] enables us to harvest a relatively homogeneous population of cells by LCM and a confirmation method that we harvested distal bronchiolar epithelium, the expression of Clara cell-specific protein (CCSP). In these studies, CCSP expression was more than 6,000-fold higher in LCM-retrieved bronchiolar epithelium compared to that in whole lung homogenate (data not shown). Although the sample was highly enriched in Clara cells, it should be noted that LCM harvests all the cells present at a given site. Thus, migrating inflammatory cells within the bronchiolar epithelium may have influenced the changes in gene expression. However, we detected minimal, if any, Gr-1 stained neutrophils within the bronchiolar epithelial region following 10 days of repeated CS exposure (data not shown). These data suggest that the cytokine expression in the LCM-retrieved samples were derived from the airway epithelium.

The present study indicates that the acute effects of single CS exposure cannot easily be extrapolated to the effects of repeated smoking for short or long term. The effects of CS exposure on bronchiolar epithelial cells over time may result from several processes having different time frames: (a) direct toxic interaction with constituents of CS (including free radicals) that have penetrated the protective antioxidant shield of epithelial lining fluid [41]; (b) damage to cells by toxic reactive products such as hydrogen peroxide generated by interaction between CS and epithelial cells [42] or epithelial lining fluid, which contains oxidized proteins, such as oxidized glutathione and

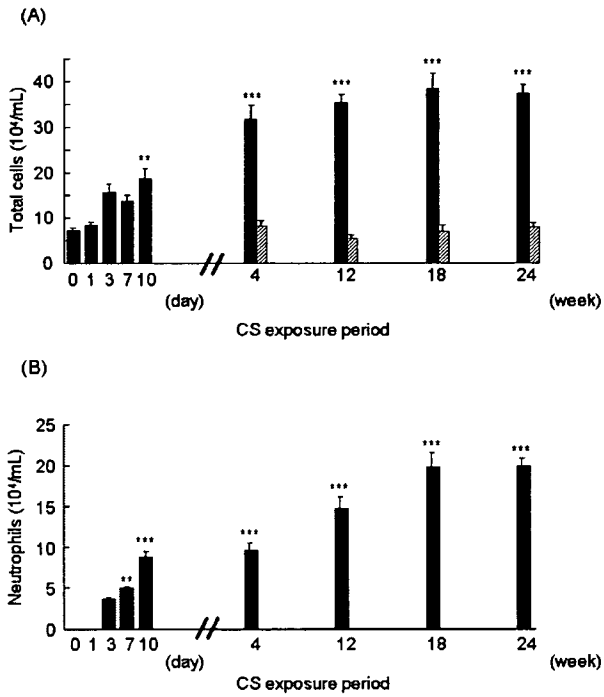

Figure 7
Long-term of CS exposure induces inflammatory cell recruitment. Mice were exposed to CS *(black bars)* or to air *(hatched bars)* for 4, 12, 18 and 24 weeks, and the cell content in the BAL fluid was identified as described in Materials and Methods. Data represent the average number of total cells *(A)* and neutrophils *(B)* per ml BAL fluid ± SEM from eight mice. The data set of Fig. 3A and 3C are also included for comparison. Statistical significance: * = $p < 0.05$; ** = $p < 0.01$; *** = $p < 0.001$ vs. before CS exposure at day 0.

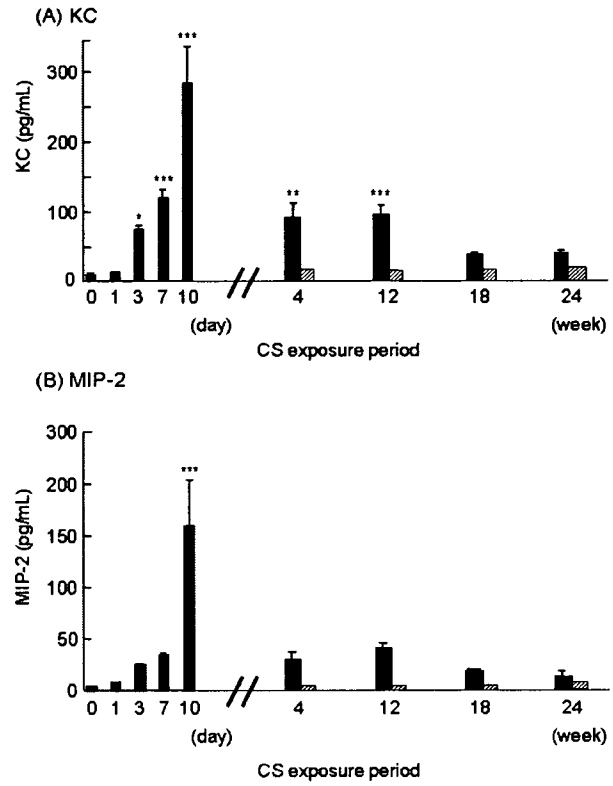

Figure 8
Long-term of CS exposure does not enhance KC and MIP-2 in BAL fluid. Mice were exposed to CS *(black bars)* or to air *(hatched bars)* for 4, 12, 18 and 24 weeks and the levels of KC *(A)* and MIP-2 *(B)* in the BAL fluid were determined by ELISA. Data represent the average concentration per ml BAL fluid ± SEM from eight mice. The data set of Fig. 4A and 4B are shown for comparison. Statistical significance: * = $p < 0.05$; ** = $p < 0.01$; *** = $p < 0.001$ vs. before CS exposure at day 0.

protein carbonyls [43]; and (c) reactions occurring subsequent to the activation of inflammatory-immune processes initiated by (a) and/or (b). Bronchiolar gene expression *in vivo* may thus be affected not only by exogenous CS, but also by the local microenvironment in bronchioles, such as infiltration of inflammatory cells, which cannot be replicated *in vitro*.

CS has been implicated in initiating a lung inflammatory response by activating transcription factors, such as NF-κB and AP-1, and chromatin unwinding (histone acetylation/deacetylation), that lead to upregulation of pro-inflammatory genes [44-46]. Di Stefano *et al.* demonstrated an increase in NF-κB p65 (A) protein in bronchial epithelium from COPD patients and from smokers with normal lung function [11]. Skerrett *et al.* reported that the cell-targeted inhibition of NF-κB activation in distal airway epithelial cells under the Clara cell 10-kDa protein/uteroglobin promoter in mice suppresses the inflammatory response to inhaled lipopolysaccharide, providing direct evidence that NF-κB activation in these cells and the subsequent signal transduction play a critical role in lung inflammation *in vivo* [47]. Elizur *et al.* also demonstrated that Clara cells, a predominant cell type in the distal airways of mice, were the predominant source of KC and MCP-1 in the early response to lipopolysaccharide [48]. In the present study, we observed 8-OHdG formation, a major reactive oxygen species (ROS)-induced DNA stress product, at 1 hr, but not 24 hr after single exposure to CS (Figure 2), which was mirrored by the expression pattern of KC and MIP-2 by bronchiolar epithelial cells (Figure 6). These data suggest that bronchiolar epithelial cells are capable of repairing oxidative DNA stress rapidly, and the temporal DNA stress in bronchiolar epithelial cells is involved in the rapid surge of KC and MIP-2 induction

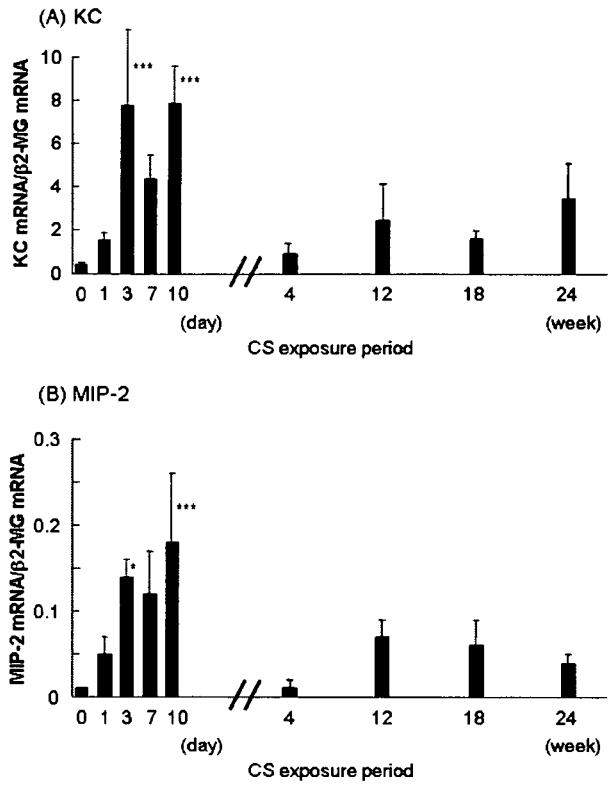

Figure 9
Long-term CS exposure dampens KC and MIP-2 expressions in LCM-retrieved bronchiolar epithelium. Mice were exposed to CS for 4, 12, 18 and 24 weeks and the expression of KC *(A)* and MIP-2 *(B)* in LCM-retrieved bronchiolar epithelium *(black bars)* were determined by real-time RT-PCR. Data represent the average expression relative to β2-MG ± SEM from at least six mice. The part of data in Fig. 5A and 5B are also used for comparison. Statistical significance: * = $p < 0.05$; ** = $p < 0.01$; *** = $p < 0.001$ vs. before CS exposure at day 0.

through redox-sensitive transcription factors, such as NF-κB or AP-1. Thus, it should be further investigated how the expression of KC and MIP-2 in those cells following CS challenge is associated with activation of NF-κB and/or AP-1 *in vivo*.

There is apparently marked diversity in the mechanisms of CS-induced inflammatory responses, even between *in vitro* experiments [8,49,50], which precludes further replication of the molecular dynamics in primary cells *in vivo*. It should be noted that rapid bronchiolar induction occurs selectively for KC and MIP-2, but not for TNF-α and IL-1β in response to initial CS exposure, suggesting that these genes are regulated by diverse pathways. All of these cytokines are eventually upregulated in bronchiolar epithelium at 10 days, however, the source of those increased cytokines in BAL fluid would become more complex at later time points, considering many other cell types involved.

In the 10 consecutive day CS exposure experiments, we have found that the response of bronchiolar epithelium to CS varies depending on prior exposure. There are marked differences in the response of the distal airway epithelial cells elicited by the very first CS exposure compared to what happens after repeated CS exposure. After repeated CS exposures, we did not detect DNA oxidative stress or a surge in KC and MIP-2 expression. These data suggest that repeated CS exposure elicits a mechanism in airway epithelial cells to protect against DNA oxidative stress, which in turn affects redox-mediated cytokine production. However, although the surge of KC and MIP-2 expression in response to CS was lost, there was a continual rise in expression of KC, MIP-2, TNF-α, and IL-1β by the bronchiolar epithelial cells upon repeated CS exposure, which was mirrored by their levels in BAL fluids and the influx of neutrophils into the lung up to 10 days.

The comparison of short and long CS exposure models highlighted the complexity of the inflammatory response of the lungs to exposure to CS. The mechanisms by which the long-term CS exposure dampens bronchiolar expressions of KC and MIP-2 need further investigation. Interestingly, neutrophil accumulation in BAL fluid becomes independent of KC and MIP-2 levels during long-term CS exposure. Possible explanations are: (a) other chemoattractants, such as MIP-3α/CCL20, replace KC and MIP-2 to recruit neutrophils [51], (b) extracellular matrix fragments resulting from damage after chronic CS exposure could be pro-inflammatory [52,53], and/or (c) the partitioning of neutrophils between tissue and alveolar spaces changes, possibly due to changes in adhesion and/or development of more channels for neutrophil egress into alveolar spaces.

Taken together, the successful collection of bronchiolar epithelium by LCM and the comparative gene expression analyses has revealed the detailed kinetic profiles of cytokine expression following CS exposure in bronchiolar epithelium. Our data suggest that airway epithelial cells play a role in the recruitment of inflammatory cells in response to CS exposure, and that there are multiple mechanisms by which CS exposure induces cytokine production by bronchiolar epithelial cells. It is to be emphasized that the CS model used in this study is only intended as a bridge between *in vitro* and *in vivo* studies of neutrophil recruitment in response to CS. Extrapolations of current findings to the other experimental CS models or to the human should be made with caution.

Conclusion

In this study, we described the variable patterns of bronchiolar epithelial cytokine expression depending on the duration of CS exposure, and these findings indicate that complex mechanisms govern bronchiolar molecular dynamics *in vivo*.

Competing interests

The authors declare that they have no competing interests. The study has not been supported by tobacco industry.

Authors' contributions

TB conceived of the study, participated in its design, and drafted the manuscript. IH and HT smoked mice to CS, collected lung samples, and carried out ELISA and part of RT-PCR. JH carried out laser capture microdissection and immunohistochemistry and part of RT-PCR, and performed the statistical analysis. TA participated in the study design and drafted the manuscript. HM, RS and MN supervised the study, and helped to draft the manuscript. All authors have read and approved the final manuscript.

Acknowledgements

The authors wish to thank to Ms. Yoko Suzuki for technical assistance, and Ms. Naomi Matsui for care and treatment of the mouse CS model. This work was supported by the scientific research grants from the Ministry of Education, Science, Culture and Sports of Japan (13470125 to MN, 14570532 to TB), Francis Family Foundation (TLA-K), Teijin Pharma Ltd., NHLBI/NIH P50 HL084922 (RMS, TB), and respiratory failure research group of the Ministry of Health, Labor, and Welfare of Japan.

References

1. Jeffery PK: **Structural and inflammatory changes in COPD: a comparison with asthma.** *Thorax* 1998, **53**:129-136.
2. Saetta M, Di Stefano A, Turato G, Facchini FM, Corbino L, Mapp CE, Maestrelli P, Ciaccia A, Fabbri LM: **CD8+ T-lymphocytes in peripheral airways of smokers with chronic obstructive pulmonary disease.** *Am J Respir Crit Care Med* 1998, **157**:822-826.
3. Saetta M: **Airway inflammation in chronic obstructive pulmonary disease.** *Am J Respir Crit Care Med* 1999, **160**:S17-S20.
4. Barnes PJ: **Small airways in COPD.** *N Engl J Med* 2004, **350**:2635-2637.
5. Chung KF: **Cytokines in chronic obstructive pulmonary disease.** *Eur Respir J Suppl* 2001, **34**:50s-59s.
6. Brusselle GG, Bracke KR, Maes T, D'hulst AI, Moerloose KB, Joos GF, Pauwels RA: **Murine models of COPD.** *Pulm Pharmacol Ther* 2006, **19**:155-165.
7. Pettersen CA, Adler KB: **Airways inflammation and COPD: epithelial-neutrophil interactions.** *Chest* 2002, **121**:142S-150S.
8. van der Vaart H, Postma DS, Timens W, ten Hacken NH: **Acute effects of cigarette smoke on inflammation and oxidative stress: a review.** *Thorax* 2004, **59**:713-721.
9. Moodie FM, Marwick JA, Anderson CS, Szulakowski P, Biswas SK, Bauter MR, Kilty I, Rahman I: **Oxidative stress and cigarette smoke alter chromatin remodeling but differentially regulate NF-kappaB activation and proinflammatory cytokine release in alveolar epithelial cells.** *FASEB J* 2004, **18**:1897-1899.
10. Yang SR, Chida AS, Bauter MR, Shafiq N, Seweryniak K, Maggirwar SB, Kilty I, Rahman I: **Cigarette smoke induces proinflammatory cytokine release by activation of NF-kappaB and posttranslational modifications of histone deacetylase in macrophages.** *Am J Physiol Lung Cell Mol Physiol* 2006, **291**:L46-L57.
11. Di Stefano A, Caramori G, Oates T, Capelli A, Lusuardi M, Gnemmi I, Ioli F, Chung KF, Donner CF, Barnes PJ, Adcock IM: **Increased expression of nuclear factor-kappaB in bronchial biopsies from smokers and patients with COPD.** *Eur Respir J* 2002, **20**:556-563.
12. Bates DV: **The respiratory bronchiole as a target organ for the effects of dusts and gases.** *J Occup Med* 1973, **15**:177-180.
13. Shaw RJ, Djukanovic R, Tashkin DP, Millar AB, du Bois RM, Orr PA: **The role of small airways in lung disease.** *Respir Med* 2002, **96**:67-80.
14. Beisswenger C, Platz J, Seifart C, Vogelmeier C, Bals R: **Exposure of differentiated airway epithelial cells to volatile smoke in vitro.** *Respiration* 2004, **71**:402-409.
15. Kode A, Yang SR, Rahman I: **Differential effects of cigarette smoke on oxidative stress and proinflammatory cytokine release in primary human airway epithelial cells and in a variety of transformed alveolar epithelial cells.** *Respir Res* 2006, **7**:132.
16. Mio T, Romberger DJ, Thompson AB, Robbins RA, Heires A, Rennard SI: **Cigarette smoke induces interleukin-8 release from human bronchial epithelial cells.** *Am J Respir Crit Care Med* 1997, **155**:1770-1776.
17. de Boer WI, Sont JK, van Schadewijk A, Stolk J, van Krieken JH, Hiemstra PS: **Monocyte chemoattractant protein 1, interleukin 8, and chronic airways inflammation in COPD.** *J Pathol* 2000, **190**:619-626.
18. Fuke S, Betsuyaku T, Nasuhara Y, Morikawa T, Katoh H, Nishimura M: **Chemokines in bronchiolar epithelium in the development of chronic obstructive pulmonary disease.** *Am J Respir Cell Mol Biol* 2004, **31**:405-412.
19. Profita M, Chiappara G, Mirabella F, Di Giorgi R, Chimenti L, Costanzo G, Riccobono L, Bellia V, Bousquet J, Vignola AM: **Effect of cilomilast (Ariflo) on TNF-alpha, IL-8, and GM-CSF release by airway cells of patients with COPD.** *Thorax* 2003, **58**:573-579.
20. Suzuki M, Betsuyaku T, Nagai K, Fuke S, Nasuhara Y, Kaga K, Kondo S, Hamamura I, Hata J, Takahashi H, Nishimura M: **Decreased airway expression of vascular endothelial growth factor in cigarette smoke-induced emphysema in mice and COPD patients.** *Inhal Toxicol* in press.
21. Dhar P: **Measuring tobacco smoke exposure: quantifying nicotine/cotinine concentration in biological samples by colorimetry, chromatography and immunoassay methods.** *J Pharm Biomed Anal* 2004, **35**:155-168.
22. Betsuyaku T, Fukuda Y, Parks WC, Shipley JM, Senior RM: **Gelatinase B is required for alveolar bronchiolization after intratracheal bleomycin.** *Am J Pathol* 2000, **157**:525-535.
23. Betsuyaku T, Griffin GL, Watson MA, Senior RM: **Laser capture microdissection and real-time reverse transcriptase/polymerase chain reaction of bronchiolar epithelium after bleomycin.** *Am J Respir Cell Mol Biol* 2001, **25**:278-284.
24. Toyokuni S, Tanaka T, Hattori Y, Nishiyama Y, Yoshida A, Uchida K, Hiai H, Ochi H, Osawa T: **Quantitative immunohistochemical determination of 8-hydroxy-2'-deoxyguanosine by a monoclonal antibody N45.1: its application to ferric nitrilotriacetate-induced renal carcinogenesis model.** *Lab Invest* 1997, **76**:365-374.
25. Betsuyaku T, Senior RM: **Laser capture microdissection and mRNA characterization of mouse airway epithelium: methodological considerations.** *Micron* 2004, **35**:229-234.
26. Cataisson C, Pearson AJ, Tsien MZ, Mascia F, Gao JL, Pastore S, Yuspa SH: **CXCR2 ligands and G-CSF mediate PKCalpha-induced intraepidermal inflammation.** *J Clin Invest* 2006, **116**:2757-2766.
27. d'Empaire G, Baer MT, Gibson FC 3rd: **The K1 serotype capsular polysaccharide of Porphyromonas gingivalis elicits chemokine production from murine macrophages that facilitates cell migration.** *Infect Immun* 2006, **74**:6236-6243.
28. Nakazawa T, Nakazawa C, Matsubara A, Noda K, Hisatomi T, She H, Michaud N, Hafezi-Moghadam A, Miller JW, Benowitz LI: **Tumor necrosis factor-alpha mediates oligodendrocyte death and delayed retinal ganglion cell loss in a mouse model of glaucoma.** *J Neurosci* 2006, **26**:12633-12641.
29. Lu JY, Sadri N, Schneider RJ: **Endotoxic shock in AUF1 knockout mice mediated by failure to degrade proinflammatory cytokine mRNAs.** *Genes Dev* 2006, **20**:3174-3184.
30. Obot C, Lee K, Fuciarelli A, Renne R, McKinney W: **Characterization of mainstream cigarette smoke-induced biomarker responses in ICR and C57Bl/6 mice.** *Inhal Toxicol* 2004, **16**:701-719.

31. Jarvis MJ, Primatesta P, Erens B, Feyerabend C, Bryant A: **Measuring nicotine intake in population surveys: comparability of saliva cotinine and plasma cotinine estimates.** *Nicotine Tob Res* 2003, **5**:349-355.
32. Subramaniam S, Whitsett JA, Hull W, Gairola CG: **Alteration of pulmonary surfactant proteins in rats chronically exposed to cigarette smoke.** *Toxicol Appl Pharmacol* 1996, **140**:274-280.
33. Van Miert E, Dumont X, Bernard A: **CC16 as a marker of lung epithelial hyperpermeability in an acute model of rats exposed to mainstream cigarette smoke.** *Toxicol Lett* 2005, **159**:115-123.
34. Aoshiba K, Koinuma M, Yokohori N, Nagai A: **Immunohistochemical evaluation of oxidative stress in murine lungs after cigarette smoke exposure.** *Inhal Toxicol* 2003, **15**:1029-1038.
35. Belperio JA, Keane MP, Burdick MD, Londhe V, Xue YY, Li K, Phillips RJ, Strieter RM: **Critical role for CXCR2 and CXCR2 ligands during the pathogenesis of ventilator-induced lung injury.** *J Clin Invest* 2002, **110**:1703-1716.
36. Belperio JA, Keane MP, Burdick MD, Gomperts BN, Xue YY, Hong K, Mestas J, Zisman D, Ardehali A, Saggar R, Lynch JP 3rd, Ross DJ, Strieter RM: **CXCR2/CXCR2 ligand biology during lung transplant ischemia-reperfusion injury.** *J Immunol* 2005, **175**:6931-6939.
37. Call DR, Nemzek JA, Ebong SJ, Bolgos GR, Newcomb DE, Wollenberg GK, Remick DG: **Differential local and systemic regulation of the murine chemokines KC and MIP2.** *Shock* 2001, **15**:278-284.
38. Kubo S, Kobayashi M, Masunaga Y, Ishii H, Hirano Y, Takahashi K, Shimizu Y: **Cytokine and chemokine expression in cigarette smoke-induced lung injury in guinea pigs.** *Eur Respir J* 2005, **26**:993-1001.
39. Thatcher TH, McHugh NA, Egan RW, Chapman RW, Hey JA, Turner CK, Redonnet MR, Seweryniak KE, Sime PJ, Phipps RP: **Role of CXCR2 in cigarette smoke-induced lung inflammation.** *Am J Physiol Lung Cell Mol Physiol* 2005, **289**:L322-L328.
40. Plopper CG: **Clara cells.** In *Lung Growth and Development. Lung Biology in Health and Disease* Edited by: McDonald JA. Marcel Dekker. New York; 1997:181-209.
41. Pryor WA, Stone K: **Oxidants in cigarette smoke. Radicals, hydrogen peroxide, peroxynitrate, and peroxynitrite.** *Ann N Y Acad Sci* 1993, **686**:12-27. discussion 27–28
42. Lavigne MC, Eppihimer MJ: **Cigarette smoke condensate induces MMP-12 gene expression in airway-like epithelia.** *Biochem Biophys Res Commun* 2005, **330**:194-203.
43. Nagai K, Betsuyaku T, Kondo T, Nasuhara Y, Nishimura M: **Long term smoking with age builds up excessive oxidative stress in bronchoalveolar lavage fluid.** *Thorax* 2006, **61**:496-502.
44. Everhart MB, Han W, Sherrill TP, Arutiunov M, Polosukhin VV, Burke JR, Sadikot RT, Christman JW, Yull FE, Blackwell TS: **Duration and intensity of NF-kappaB activity determine the severity of endotoxin-induced acute lung injury.** *J Immunol* 2006, **176**:4995-5005.
45. Rahman I, Adcock IM: **Oxidative stress and redox regulation of lung inflammation in COPD.** *Eur Respir J* 2006, **28**:219-242.
46. Zhou L, Tan A, Iasvovskaia S, Li J, Lin A, Hershenson MB: **Ras and mitogen-activated protein kinase kinase kinase-1 coregulate activator protein-1- and nuclear factor-kappaB-mediated gene expression in airway epithelial cells.** *Am J Respir Cell Mol Biol* 2003, **28**:762-729.
47. Skerrett SJ, Liggitt HD, Hajjar AM, Ernst RK, Miller SI, Wilson CB: **Respiratory epithelial cells regulate lung inflammation in response to inhaled endotoxin.** *Am J Physiol Lung Cell Mol Physiol* in press.
48. Elizur A, Adair-Kirk TL, Kelley DG, Griffin GL, Demello DE, Senior RM: **Clara cells impact the pulmonary innate immune response to LPS.** *Am J Physiol Lung Cell Mol Physiol* 2007. 2007 May 25, 101152/ajplung.00024.2007
49. Hellermann GR, Nagy SB, Kong X, Lockey RF, Mohapatra SS: **Mechanism of cigarette smoke condensate-induced acute inflammatory response in human bronchial epithelial cells.** *Respir Res* 2002, **3**:22.
50. Laan M, Bozinovski S, Anderson GP: **Cigarette smoke inhibits lipopolysaccharide-induced production of inflammatory cytokines by suppressing the activation of activator protein-1 in bronchial epithelial cells.** *J Immunol* 2004, **173**:4164-4170.
51. Bracke KR, D'hulst AI, Maes T, Moerloose KB, Demedts IK, Lebecque S, Joos GF, Brusselle GG: **Cigarette smoke-induced pulmonary inflammation and emphysema are attenuated in CCR6-deficient mice.** *J Immunol* 2006, **177**:4350-4359.
52. Houghton AM, Quintero PA, Perkins DL, Kobayashi DK, Kelley DG, Marconcini LA, Mecham RP, Senior RM, Shapiro SD: **Elastin fragments drive disease progression in a murine model of emphysema.** *J Clin Invest* 2006, **116**:753-759.
53. Weathington NM, van Houwelingen AH, Noerager BD, Jackson PL, Kraneveld AD, Galin FS, Folkerts G, Nijkamp FP, Blalock JE: **A novel peptide CXCR ligand derived from extracellular matrix degradation during airway inflammation.** *Nat Med* 2006, **12**:317-323.

ANTIOXIDANTS & REDOX SIGNALING
Volume 10, Number 4, 2008

DOI: 10.1089/ars.2007.1941

Forum Original Research Communication

Dual Oxidase 1 and 2 Expression in Airway Epithelium of Smokers and Patients with Mild/Moderate Chronic Obstructive Pulmonary Disease

KATSURA NAGAI,[1] TOMOKO BETSUYAKU,[1] MASARU SUZUKI,[1] YASUYUKI NASUHARA,[1] KICHIZO KAGA,[2] SATOSHI KONDO,[2] and MASAHARU NISHIMURA[1]

ABSTRACT

Dual oxidase (Duox) 1 and Duox2 are important sources of hydrogen peroxide production and play a role in host defense in airways. Little is known about their regulation in association with smoking or chronic obstructive pulmonary disease (COPD). We investigated the epithelial expression of Duox1 and Duox2 in the airways of smokers, and the relationship between this expression and COPD at early stage. First, using bronchoscopy, we harvested tracheal and bronchial epithelium from individuals who have never smoked and current smokers. Duox1 expression in brushed tracheal and bronchial epithelium was significantly downregulated, whereas Duox2 was upregulated, in current smokers as compared to individuals who have never smoked. Second, laser capture microdissection and microscope-assisted manual dissection were performed in surgically resected lung tissues to collect bronchiolar epithelium and alveolar septa. Subjects with mild/moderate COPD, who were all former smokers, exhibited downregulation of bronchiolar Duox1 and Duox2 when compared to individuals who have never smoked, whereas a difference between former smokers, with and without COPD, was observed only for Duox1. Alveolar Duox1 and Duox2 expression was low and did not differ among the groups. These results imply that the airway expression of Duox1 and Duox2 is diversely associated with smoking and COPD. *Antioxid Redox Signal* 10, 705–714.

INTRODUCTION

PARTIALLY REDUCED METABOLITES OF MOLECULAR OXYGEN, superoxide and hydrogen peroxide (H_2O_2), are detected in respiratory tract lining fluid, and it is assumed that these are key components of innate immunity (43). Phagocytic cells produce by the nicotinamide adenine dinucleotide phosphate (NADPH) oxidase system, which contributes to the killing of invading microorganisms. Dual oxidase (Duox), a newly identified NADPH oxidase homolog, is expressed in the barrier epithelia, including epithelial surfaces of colon, rectum, salivary gland ducts, and bronchi (9, 11, 15). Adult flies in which *Drosophila* Duox expression is silenced have a markedly increased mortality rate after a minor infection caused by the ingestion of microbe-contaminated food; this finding suggests that Duox plays an indispensable role in antimicrobial activities (16). Duox contains two well-characterized domains, an NADPH oxidase domain and a heme peroxidase domain (7). The two isoforms of Duox, Duox1 and Duox2, share >83% sequence homology at the amino acid level (4). Duox1 is constitutively expressed in ciliated epithelium along the respiratory tract (11, 15, 33), although Duox2 expression is inducible in response to exogenous stimuli (17). Both Duox1 and Duox2 expressions are calcium dependent (6, 8). Duox1 mRNA expression is modestly upregulated in response to Th2-specific cytokines interleukin (IL)-4 and IL-13, whereas Duox2 mRNA expression is markedly induced by the Th1-specific cytokine interferon-γ (IFN-γ) (17, 18). However, many questions remain

[1]First Department of Medicine and [2]Department of Surgical Oncology, Hokkaido University School of Medicine, Sapporo, Japan.

regarding the regulation and function of each Duox isoform in human airway epithelium.

ROS has been suggested to play a role in smoking-induced COPD (31). ROS could be exogenously driven by air pollutants or cigarette smoke, or endogenously produced through metabolic reactions (32). The sources of ROS in patients with COPD have been thought to be not only cigarette smoke itself, but also increased inflammatory cells such as leukocytes and macrophages (25) in the lungs, where NADPH oxidase is one of the key enzymes to generate ROS. We speculate that newly identified epithelial Duox may contribute to the generation of endogenous ROS in airway epithelial cells. Cigarette smoke exposure elicits a variety of stimuli on airway epithelium. COPD associated with chronic cigarette smoking eventually involves all levels of the airways, although the earliest smoking-induced changes occur in the small airway epithelium (19, 37). So far, it remains to be elucidated whether Duox1 and Duox2 are differently regulated by chronic smoking *in vivo* and whether the changes in their gene expression are associated with COPD. Therefore, in the present study we compared the mRNA expression of Duox1 and Duox2 in tracheal and bronchial epithelial cells, which were harvested by bronchoscopic brushing, from individuals who have never smoked and age-matched, healthy, current smokers. Second, to study the roles of Duox1 and Duox2 in the pathophysiology of COPD, the Duox1 and Duox2 mRNA expression levels were examined in bronchiolar epithelial cells and alveolar septa from individuals who have never smoked and former smokers with and without COPD.

MATERIALS AND METHODS

Subjects

We recruited two sets of subjects: one set for the bronchoscopic study and the other set for the surgical tissue study. For the bronchoscopic study, tracheal and bronchial epithelial cells were harvested by brushing, and epithelial lining fluid was collected by microsampling (20, 45). The bronchoscopic study had 11 subjects, consisting of 6 individuals who have never smoked and 5 healthy current smokers. All healthy current smokers abstained from smoking for 12 h prior to bronchoscopy in order to maintain a consistent amount of time from the last exposure to cigarette smoke.

Thirty patients who had lung resection for small peripheral tumors were recruited for the surgical tissue study. Ten were individuals who have never smoked, 10 were former smokers without COPD (smoking cessation; 7 days to 27 years), and 10 were former smokers with COPD (smoking cessation; 5 days to 9 years). The subjects with COPD were classified according to the guidelines of the Global Initiative for Obstructive Lung Disease (GOLD) (10) into stage I ($n = 8$) and stage II ($n = 2$). Eight subjects had emphysema on computed tomography scans, including the two subjects with stage II COPD. Two subjects with stage I COPD had no emphysema on computed tomography scans. Some patients were subjects in our previous study (14).

For both studies, pulmonary function tests were performed as previously described (26). None of the subjects had a history of asthma or other allergic disorders; also, none of the subjects had a chronic productive cough. All subjects gave written informed consent, and the study was approved by the Ethics Committee of Hokkaido University School of Medicine, Sapporo, Japan.

Collection of tracheal and bronchial epithelial cells by bronchoscopic brushing

Bronchoscopic brushing was conducted through a flexible fiberoptic bronchoscope (Model BF-1T200; Olympus, Tokyo, Japan) to collect tracheal and bronchial epithelial cells around carina and at the fourth or fifth branches of subsegmental lower lobe bronchus, respectively. The cells were immediately collected by vortexing the brush in RPMI 1640 medium (GIBCO, Grand Island, NY). The cells were centrifuged for 5 min at 1,000 rpm, and the red blood cells were removed with red blood cell lysing buffer (Sigma, St. Louis, MO). The recovered cells were washed twice in Hanks' balanced salt solution without calcium and magnesium (Gibco). The cytospin preparations were stained by Diff-Quik stain (Kokusai Shiyaku, Kobe, Japan). Differential counts were performed by examining >300 cells, using a standard light microscope as previously described (2). For detection of keratin in the cells, the specimens were stained with antikeratin antibody (KL-1; Immunotech, Marseille, Cedex, France). The cytospin preparations were also stained by periodic acid-Schiff (PAS) stain for the detection of secretory granules. Cells were adjusted to 1×10^6/ml and used for preparation of total RNA.

Collection of epithelial lining fluid by bronchoscopic microsampling

During bronchoscopy, microsampling was performed as previously described (20), with slight modification prior to the brushing procedure. Using a special cotton probe (model BC-402C, Olympus), sampling of epithelial lining fluid was repeated three times at sites adjacent to the location of brushing. The absorbed epithelial lining fluid (using three microsampling probes per given site) was extracted into 3 ml of saline and the mean weight of lining fluid per probe was calculated as previously described (20).

Quantification of IFN-γ in epithelial lining fluid

IFN-γ was quantified using a human IFN-γ enzyme-linked immunoassay kit II (BD Biosciences, San Diego, CA) according to the supplied protocol. A standard curve was obtained by log–log using serial dilutions of the supplied recombinant IFN-γ (minimal detection limit 1 pg/ml). The concentrations of IFN-γ were converted using the respective dilution factors and were expressed as those in epithelial lining fluid, as previously described (20).

Sampling of bronchiolar epithelial cells, alveolar septa for lung specimen

Six or more blocks of peripheral lung tissue were collected in areas remote enough from the tumors and were frozen. Laser capture microdissection (LCM) of bronchiolar epithelial cells was performed by using a PixCell II System (Arcturus Engineering, Mountain View, CA) (Figs. 1a, b, and c), as described

previously (14). At least six bronchioles were randomly selected, and a total of 40,000 laser bursts were used to collect cells from each subject. Alveolar septa were identified, and adjacent unwanted tissues were removed using an 18-gauge fine sterile needle; the remaining tissue was harvested from hematoxylin-stained lung sections (Figs. 1d, e, and f).

RNA purification and quantitative reverse transcriptase-polymerase chain reaction (RT-PCR)

We used the epithelial cell samples collected by bronchial brushing for RT-PCR only when the samples contained <5%

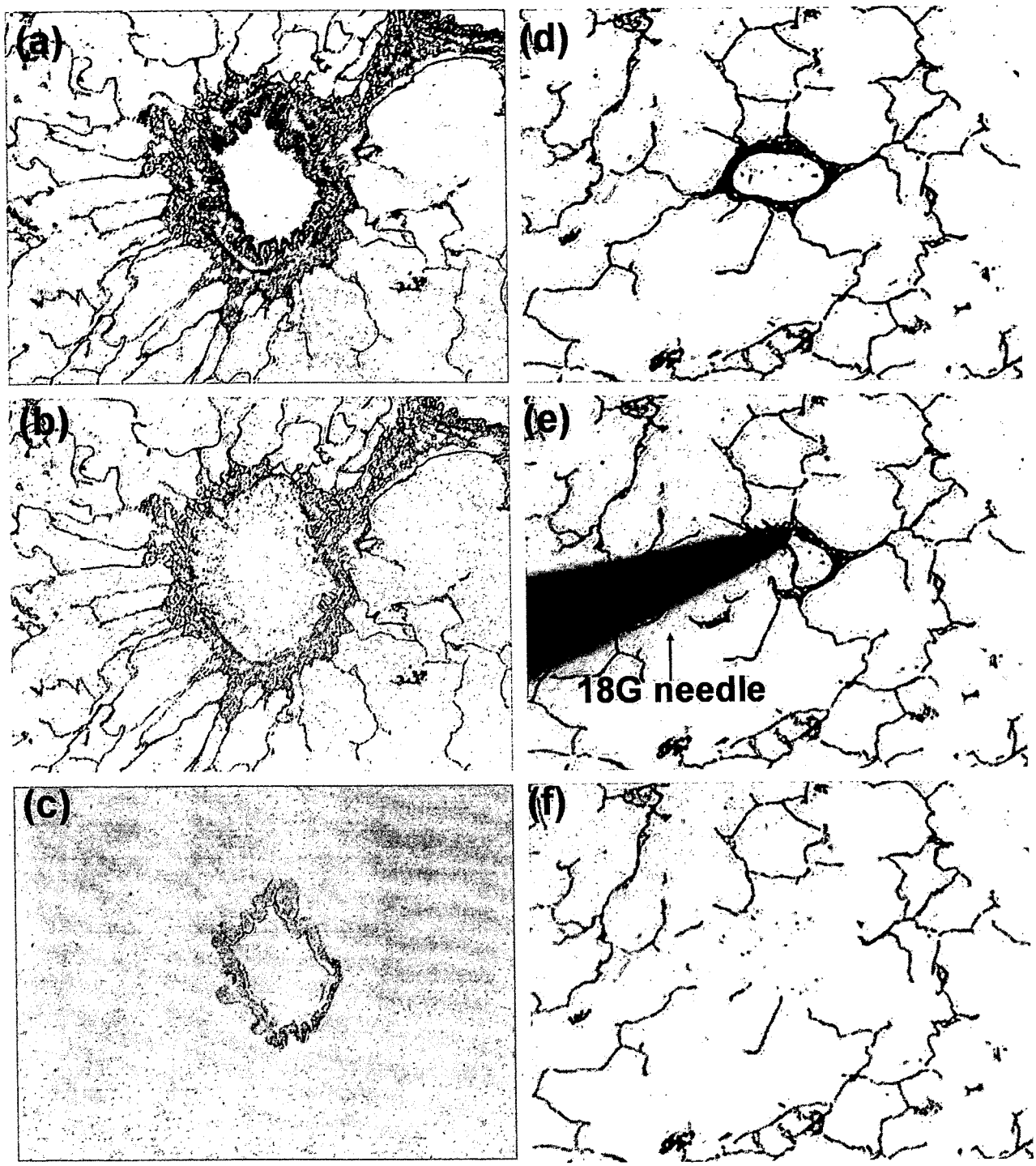

FIG. 1. Sampling of bronchiolar epithelial cells, alveolar septa for lung specimen. Lung tissue section (**a**) before and (**b**) after laser capture microdissection of bronchiolar epithelial cells, and (**c**) captured bronchiolar epithelium cells on a transfer film. Lung tissue sections (**d**) before dissection, (**e**) manual dissection of unwanted tissue, and (**f**) remained alveolar tissue.

nonepithelial cells, as determined by Diff-Quik staining and keratin staining. Total RNA was extracted by using an RNeasy mini kit (Qiagen, Hilden, Germany) with guanidium thiocyanate. The quantity and quality of the RNA were determined by using a LabChip kit (Agilent Technologies, Palo Alto, CA). Reverse transcription was performed in the presence of Maloney leukemia virus reverse transcriptase (Epicentre Technologies, Madison, WI), and 5′ exonuclease-based fluorogenic PCR was performed with an ABI PRISM 7700 Sequence Detector (Applied Biosystems, Foster City, CA), as described previously (1). TaqMan Gene Expression Assay probes (Applied Biosystems) were used for the human Duox1 (Hs00213694_m1, GenBank accession number NM 000619) and Duox2 gene sequence (Hs00204187_m1, GenBank accession number NM 014080), and the levels were normalized against glyceraldehyde-3-phosphatase-dehydrogenase (GAPDH) mRNA.

Data presentation and statistical analysis

Demographic data were expressed as means ± standard error (SE). Data were analyzed by using an unpaired *t* test for the bronchoscopic study. For the surgical tissue study, a single factor analysis of variance followed by Fisher's protected least significant difference test as a *post hoc* test. The other data were expressed as median and range, considering that the values in each group were widely ranged and not evenly distributed. Differences between two groups were analyzed by using the Mann–Whitney U test, and more than two groups were compared by using the Kruskal–Wallis test, followed by the Mann–Whitney U test. All tests were performed using the StatView J 5.0 System (SAS Institute Inc., Cary, NC). P values <0.05 were considered statistically significant.

RESULTS

Subjects

Eleven subjects underwent bronchoscopy for epithelial brushing and microsampling. There was no difference in age between the individuals who have never smoked and the current smokers (68 ± 3 *vs.* 61 ± 2 years, mean ± SE). The number of pack-years of smoking for the current smokers was 48 ± 9 (mean ± SE). All subjects had normal pulmonary function tests. There was no difference between the individuals who have never smoked and current smokers in the percent predicted value of the forced expiratory volume in one second (FEV_1;122 ± 10% *vs.* 112 ± 11%) and in FEV_1/forced vital capacity (79 ± 4% *vs.* 78 ± 2%).

The clinical characteristics of the subjects enrolled and the pathological diagnosis of the resected tumors in the surgical tissue study are summarized in Table 1. Both groups of former smokers (with and without COPD) had a similar number of pack-years of smoking; these two groups had various durations of smoking and cessation.

Differential cell counts for brushed epithelial cells

The percentage of epithelial cells was no <95% for all specimens. The total cell number, viability, and cell differential counts were not statistically different at either site between individuals who have never smoked and current smokers (Table 2). Cell viability did not differ between the two groups either at the trachea (43 ± 4% *vs.* 31 ± 7%, NS) or at the subsegmental bronchus (31 ± 3% *vs.* 23 ± 2%, NS). Very few PAS-positive epithelial cells were observed at either site in individuals who have never smoked and current smokers.

Duox1 and Duox2 mRNA expression are differently regulated in large airways of current smokers

To investigate the effects of current smoking on the transcriptional regulation of Duox1 and Duox2 in airway epithelial cells *in vivo*, we examined these mRNA expression levels in epithelial cells harvested by bronchoscopic brushing. We compared these levels between the six individuals who have never smoked and the five healthy, current smokers. Duox1 expression was significantly downregulated in the current smokers, as

TABLE 1. CLINICAL CHARACTERISTICS OF SUBJECTS IN THE SURGICAL TISSUE STUDY

	Individuals who have never smoked	*Former smokers without COPD*	*Former smokers with COPD*
n (M/F)	10 (2/8)	10 (7/3)	10 (8/2)
Age (yr)	62 ± 5	63 ± 6	70 ± 2
Pack-years	0	54 ± 15	68 ± 11
FEV_1/FVC (%)	81 ± 2	81 ± 2	62 ± 2*†
FEV_1 (% predicted value)	114 ± 6	115 ± 7	95 ± 6*†
Pathological diagnosis of resected tumor	8 adenocarcinoma 1 carcinoma of cystic dust 1 osteosarcoma	6 adenocarcinoma 2 squamous cell carcinoma 2 small cell carcinoma	6 adenocarcinoma 3 squamous cell carcinoma 1 large cell carcinoma

*$p < 0.05$ *vs.* individuals who have never smoked; †$p < 0.05$ *vs.* former smokers without COPD; FVC, forced vital capacity; FEV_1, forced expiratory volume in one second.

Data are presented as mean ± SE.